# Drivers of the projected changes to the Pacific Ocean equatorial circulation

Alexander Sen Gupta, Alexandre Ganachaud, S. Mcgregor, Jaclyn Brown, Les Muir

# Drivers of the projected changes to the Pacific Ocean equatorial circulation

A. Sen Gupta,[1] A. Ganachaud,[2,3] S. McGregor,[1] J. N. Brown,[4] and L. Muir[5]

Received 27 February 2012; revised 4 April 2012; accepted 9 April 2012; published XX Month 2012.

[1] Climate models participating in the third Coupled Model Inter Comparison Project (CMIP3) suggest a significant increase in the transport of the New Guinea Coastal Undercurrent (NGCU) and the Equatorial Undercurrent (EUC, in the central and western Pacific) and a decrease in the Mindanao current and the Indonesian Throughflow. Most models also project a reduction in the strength of the equatorial Trade winds. Typically, on ENSO time scales, a weakening of the equatorial easterlies would lead to a reduction in EUC strength in the central Pacific. The strengthening of the EUC projected for longer timescales, can be explained by a robust projected intensification of the south-easterly trade winds and an associated off-equatorial wind-stress curl change in the Southern Hemisphere. This drives the intensification of the NGCU and greater water input to the EUC in the west. A 1½-layer shallow water model, driven by projected wind stress trends from the CMIP3 models demonstrates that the projected circulation changes are consistent with a purely wind driven response. While the equatorial winds weaken for both El Niño events and in the projections, the ocean response and the mechanisms driving the projected wind changes are distinct from those operating on interannual timescales. **Citation:** Sen Gupta, A., A. Ganachaud, S. McGregor, J. N. Brown, and L. Muir (2012), Drivers of the projected changes to the Pacific Ocean equatorial circulation, *Geophys. Res. Lett.*, *39*, LXXXXX, doi:10.1029/2012GL051447.

## 1. Introduction

[2] The equatorial Pacific Ocean is a region of great importance for the global carbon cycle. It is a major region of $CO_2$ outgassing related to the re-emergence of relatively old $CO_2$-rich water [*Feely et al.*, 2006]. It also has relatively high concentrations of upwelled macro-nutrients, in the central and eastern region, that maintain large rates of new production, although these rates are limited by a lack of bioavailable iron [e.g., *Coale et al.*, 1996]. Both the $CO_2$-rich water and the iron that maintains the high productivity are derived from upwelled water from the Equatorial Undercurrent (EUC). High concentrations of iron appear to be entrained into the New Guinea Coastal Undercurrent (NGCU) a feeder to the EUC, along the continental slope of Papua New Guinea [*Mackey et al.*, 2002]. Interannual variability in the strength of the NGUC (primarily related to ENSO) and the associated entrainment of iron has been linked to phytoplankton blooms in the equatorial Pacific that can increase equatorial chlorophyll levels by a factor of three to four [*Ryan et al.*, 2006]. Upwelling variability from the EUC in the eastern Pacific also dramatically alters the $CO_2$ air-sea flux [*Feely et al.*, 2006]. As such, any future changes in the equatorial circulation may significantly alter biological productivity and carbon cycling in the region.

[3] The EUC forms a remarkably long and narrow eastward ribbon of water that spans the Pacific basin, constrained by the Coriolis force to sit on the equator. The EUC is fed, at its initiation, by equatorward flowing low-latitude western boundary currents, in particular the NGCU and the Mindanao Current. It is strengthened by a thermocline convergence within the interior [*Johnson and McPhaden*, 1999]. The equatorward transport constitutes the lower branches of the Subtropical Cells (STC) in which water subducted in the eastern extratropical Pacific, in both hemispheres, moves equatorward into the EUC [*Tsuchiya et al.*, 1989]. This water is subsequently upwelled in the central and eastern equatorial Pacific and flows southward again in the surface Ekman layer.

[4] Linear theory suggests a relationship between the equatorial wind strength and the EUC strength [*McPhaden*, 1993]. Using a reconstruction of EUC strength based on the TAO array, *Izumo* [2005] shows that weakened equatorial winds in the western and central basin excite Kelvin waves that reduce the EUC strength to the east of the wind anomalies. We find a similar relationship also exists in the CMIP3 climate models (discussed below).

[5] Projections for ENSO behaviour, however, diverge considerably across the models [e.g., *Collins et al.*, 2010]. Despite this several aspects of background-state changes pertinent to tropical circulation, are quite robust. For example, theoretical arguments [e.g., *Held and Soden*, 2006], climate model projections and recent observations [e.g., *Vecchi and Soden*, 2007] suggest that the equatorial easterlies should weaken as the troposphere warms. There is also considerable agreement with regards to a projected intensification of SE Trade Winds and a weakening of the NE Trade Winds [*Ganachaud et al.*, 2011].

[6] The weakened projected equatorial winds directly drive a weakening of the westward surface flow. In contrast, a strengthening of the EUC in the western and central Pacific

[1]Climate Change Research Centre, University of New South Wales, Sydney, New South Wales, Australia.
[2]LEGOS, UMR5566, Institut de Recherche pour le Développement, Nouméa, New Caledonia.
[3]LEGOS, UPS, OMP-PCA, Toulouse, France.
[4]Centre for Australian Weather and Climate Research, CSIRO Wealth from Oceans National Research Flagship, Hobart, Tasmania, Australia.
[5]Department of Geology and Geophysics, Yale University, New Haven, Connecticut, USA.

Corresponding Author: A. Sen Gupta, Climate Change Research Centre, University of New South Wales, Sydney, NSW 2052, Australia. (a.sengupta@unsw.edu.au)


0094-8276/12/2012GL051447

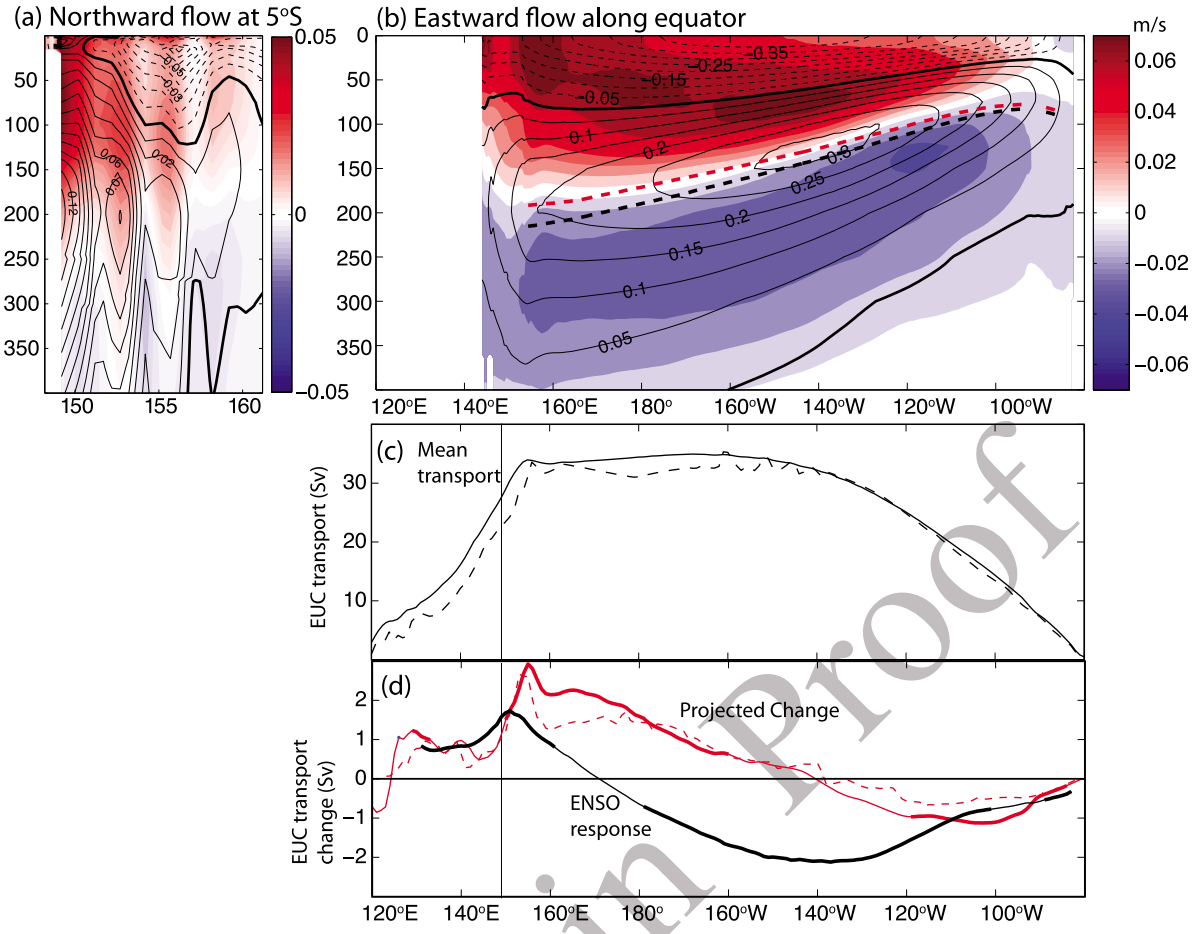


**Figure 1.** (a) Multi-model mean meridional velocity (lines) and change (shading) in meridional velocity at 5S off the coast of PNG (longitudes have been offset in individual models so that the coast of PNG lies at the same longitude). (b) Multi-model mean zonal velocity (lines) and change in zonal velocity averaged between 3S and 3N; dashed blue and red lines indicate the position of the EUC core in the 20th and 21st century, respectively (calculated as the zonal current weighted depth at each longitude). (c) Multi-model mean (continuous) and median (dashed) EUC transport. (d) Projected multi-model mean (continuous) and median (dashed) change in EUC transport (red) and 20th century EUC transport regressed onto ENSO index (black). Thickened line indicates longitudes where change is significant at 90% level.

is projected over the next century [*Ganachaud et al.*, 2012; *Luo et al.*, 2009], apparently at odds with the observed relationship between the equatorial Trades and EUC strength evident on interannual timescales [*Izumo*, 2005]. This study examines the projected changes to the equatorial circulation and the drivers of NGCU and EUC changes.

## 2. CMIP3 Simulations

[7] To examine changes in ocean and atmosphere properties we use output from the third Coupled Model Inter-comparison Project (CMIP3) [*Meehl et al.*, 2007]. Mean-state properties (based on the last 50 years of the 20th century) are compared with changes over the full 21st century for the SRES A1B scenario. To minimise aliasing by natural variability, we calculate linear trends in the properties over the 21st century and present results as the change per century. Model drift may affect the magnitude of the projected changes [*Sen Gupta et al.*, 2009, 2012] as such trends in ocean properties for individual models have been de-drifted, where possible, by subtracting any concurrent linear trends in the pre-industrial control simulation. For each scenario and model we use only a single ensemble member. For each property examined we use the maximum number of models available, except for the GISS ER model that was excluded for its inability to produce any ENSO-like variability [*Ganachaud et al.*, 2011; *Irving et al.*, 2011]. Inconsistencies in output availability, mean that analyses of different properties are made using slightly different subsets of models (Figure 2). Using a smaller set of consistent models does not substantively change our results.

## 3. Projected Changes to the Equatorial Circulation

[8] All models show some degree of upward movement of the EUC core, with almost all models exhibiting greatest shoaling towards the west (Figure 1b). In the multi-model mean, the EUC core shoals by ~25 m in the western basin decreasing to ~5 m shoaling in the eastern basin. This shoaling manifests as an eastward flow anomaly above the mean EUC core depth and a westward anomaly below

(Figure 1b). However, the acceleration of the flow above the core overwhelms the deceleration below in the western and central basin, leading to an overall intensification of the EUC, in most models. The region of strongest EUC transport in the western basin is enhanced by the largest amount ~3 Sv or +10%, in the multi-model mean (Figure 2). While there is a significant increase in EUC transport west of ~160°W, there is a weak but significant reduction in transport east of ~240°E (Figure 1d). This must result from weaker meridional pycnocline convergence and/or weaker upwelling in the eastern basin.

[9] In the multi-model-mean the NGCU, at 5°S, has a core between 150 and 250 m, consistent with observations [*Kuroda*, 2000], with a poleward flow extending from the surface to ~400 m (Figure 1a). The multi-model mean flow (24 Sv) is within the range of observational estimates [*Cravatte et al.*, 2011] (13.5 Sv down to 300 m in the Solomon straits [*Ueki*, 2003], 27 Sv down to 500 m). In some models the NGCU does not abut the coastal margin leading to local maxima situated away from the western boundary in the model mean (and the projections). There is a robust projected intensification of the NGCU in the upper 250 m (with little change or a weak deceleration at greater depth) with almost unanimous model agreement at both 9°S and 5°S (Figure 2b). In the multi-model mean, there is a ~4 Sv (+17%) increase in NGCU transport, although considerable model spread exists in the mean transport and the projected change. The enhanced input of water from the NGCU towards the equator is consistent with the large projected increase in EUC transport between 150 and 160°E.

[10] In the northern hemisphere there is no significant projected change in the southward western boundary transport at 5 N (Figure 2b), which in the mean state contributes to the EUC. There is however a significant decrease in the southward transport at 9 N and in the transport passing through the Indonesian Throughflow (ITF, of between 1 and 1.5 Sv, Figure 2b).

## 4. Mechanisms to Explain Projected Changes

[11] Figure 3a shows the projected multi-model change to the wind-stress. Most models project a strengthening of the southeast Trade winds and a weakening of the northeast and equatorial Trades. This leads to robust wind-stress curl anomalies: a strong negative anomaly is projected across much of the basin to the south of the equator at the boundary of the increasing south-easterly trades and decreasing equatorial trades with a less extensive negative curl anomaly at ~10°N. The pattern of projected equatorial trade wind decrease is model dependent but is not systematically larger in the west, as is the case during El Niños. In fact, greatest model agreement is with respect to a decrease in the eastern basin, where there is typically little wind response during ENSO events (Figure 3b).

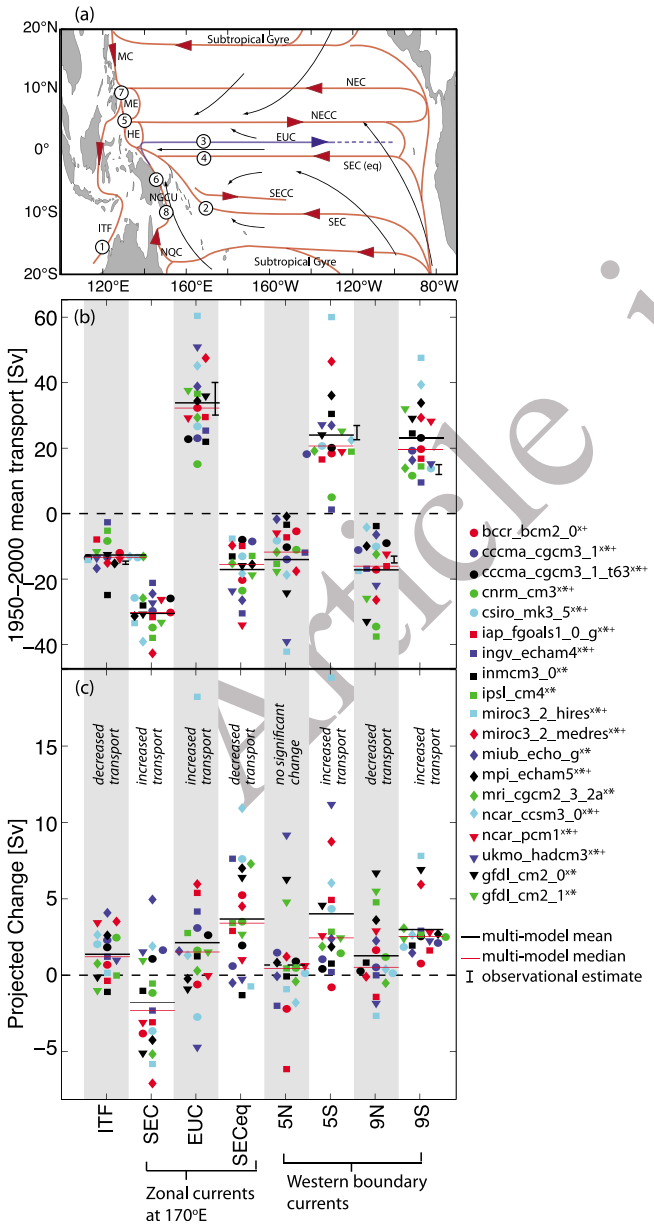


**Figure 2.** (a) Major tropical Pacific currents (red: surface, blue: sub-surface, black: mean surface winds). (b) Mean-state (1950–2000) transport for major tropical currents (Indonesian Throughflow, ITF, South Equatorial Current, SEC, Equatorial Undercurrent, EUC; equatorial South Equatorial Current, SECeq, Mindanao Current at 5N and 9N, and New Guinea Coastal Undercurrent at 5S and 9S). Currents are calculated at locations shown in Figure 2a. Coloured markers show transport from individual models, horizontal black (red) lines represent multi-model mean (median) transport. (c) As Figure 2b for projected change in transport over the 21st century. Multi-model mean changes are significant at the 90% level, except for the poleward flow at 5N. Current locations can vary considerably between models. As a result, current definitions are model specific; model velocity fields were manually examined to determine mean-state boundaries (latitudes, longitudes and depths) of the different currents. Transports are then computed from the area integrated velocity flowing in the direction of the specific current, using annual averaged data. (Observational estimates from *Butt and Lindstrom* [1994], *Gouriou and Toole* [1993], *Huang and Liu* [1999], *Izumo* [2005], *Lukas et al.* [1991], *Wijffels* [1993], *Delcroix et al.* [1992], and *Ueki* [2003].) Notes: x, models used in Figures 2, 3a, and 3b; *, models used in Figure 4; +, models used in Figure 3d.

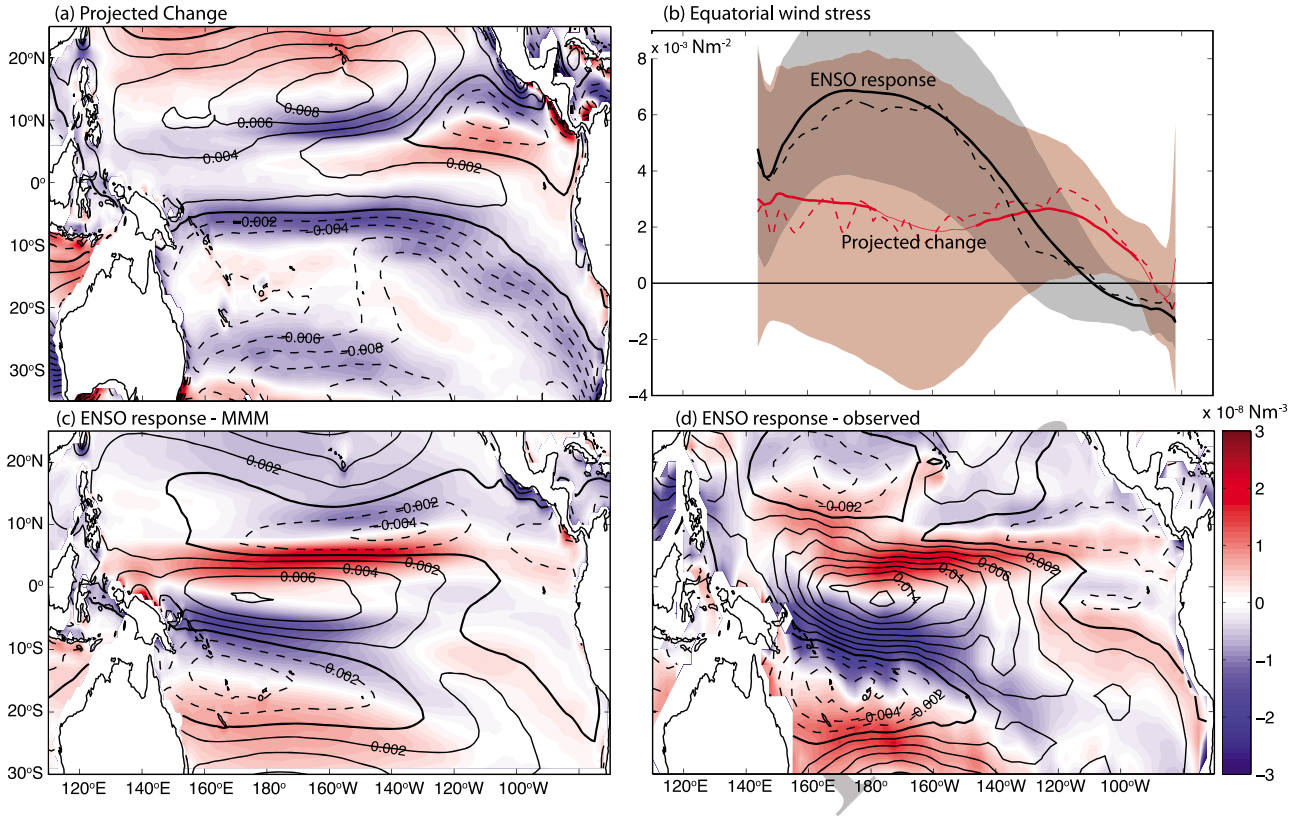


**Figure 3.** (a) Multi-model mean projected change. in zonal wind-stress (contours) and wind-stress curl (shading). (b) Multi-model mean zonally averaged (3S to 3N) projected wind stress change (solid red line) and regression of wind-stress onto ENSO index (solid black line). Thick red line indicates longitudes where the projected changes are significant at 95% level (t-test). Dashed lines show multi-model median results. Shaded regions indicate 1 standard deviation model spread about the multi-model means. (c) Multi-model mean regression of the mean zonal wind-stress (contours) and wind-stress curl (shading) on ENSO index (line contours; continuous-positive, dashed-negative, thickened-zero). (d) As Figure 3c for observations based on ECMWF [*Uppala et al.*, 2005], and HadISST [*Rayner et al.*, 2003], products. (Regression units, wind-stress: 10–3 Nm-2/standard deviation; wind-stress curl: 10–8 Nm-3/standard deviation.)

[12] The projected equatorial wind-stress reduction is small compared to a typical (one standard deviation) El Niño event over most of the basin (Figure 3b). However the projected wind-stress curl change in the southern hemisphere is of a similar magnitude (and latitude) to a wind-stress curl anomaly typical of a one-standard deviation El Niño, but extends over a greater zonal extent (Figures 3a and 3c). In the northern hemisphere the projected change to the curl is of the opposite sign (i.e., a negative change) to an El Niño-related anomaly and is situated considerably further north.

[13] For interannual timescales *Lee and Fukumori* [2003] separate the tropical circulation response onto a part driven by changes to the equatorial zonal wind-stress and a part related to the off-equatorial wind stress curl. These two processes operate together to modulate the equatorial circulation response to ENSO or Pacific decadal variability. For example, during an El Niño, the reduced equatorial easterlies in the western basin, are associated with flanking positive (negative) wind stress curl anomalies in the northern (southern) hemispheres (Figure 3). *Lee and Fukumori* [2003] show that the decreased equatorial wind-stress reduces the strength of STCs: the Ekman divergence, the compensating interior equatorward pycnocline convergence and the EUC that links the upper and lower STC branches. On the other hand, the flanking curl anomalies drive an increased equatorward boundary transport and a compensating reduced interior pycnocline convergence. The net effect is an increase in EUC transport in the far western basin (driven by enhanced boundary flow), but a more pervasive decrease in transport over the rest of the basin. Such a change is evident in the mean CMIP3 model response to ENSO (Figure 1d). Using an ocean model forced with historical winds *Capotondi et al.* [2005] also demonstrate a strong compensation between interior and western boundary flow at both interannual and decadal timescales. They highlight how baroclinic Rossby wave adjustment to the wind stress changes act to set up the observed circulation changes.

[14] The projected EUC and NGCU changes can also be understood in terms of the on- and off-equatorial processes described above. The strong projected negative wind-stress curl anomaly in the Southern Hemisphere causes an intensification of the NGUC with a compensating reduction in the interior pycnocline convergence. This drives the projected EUC intensification in the west (Figure 1d). The weak projected reduction in the equatorial trades additionally forces a weak overall slowdown of the EUC. The relatively large

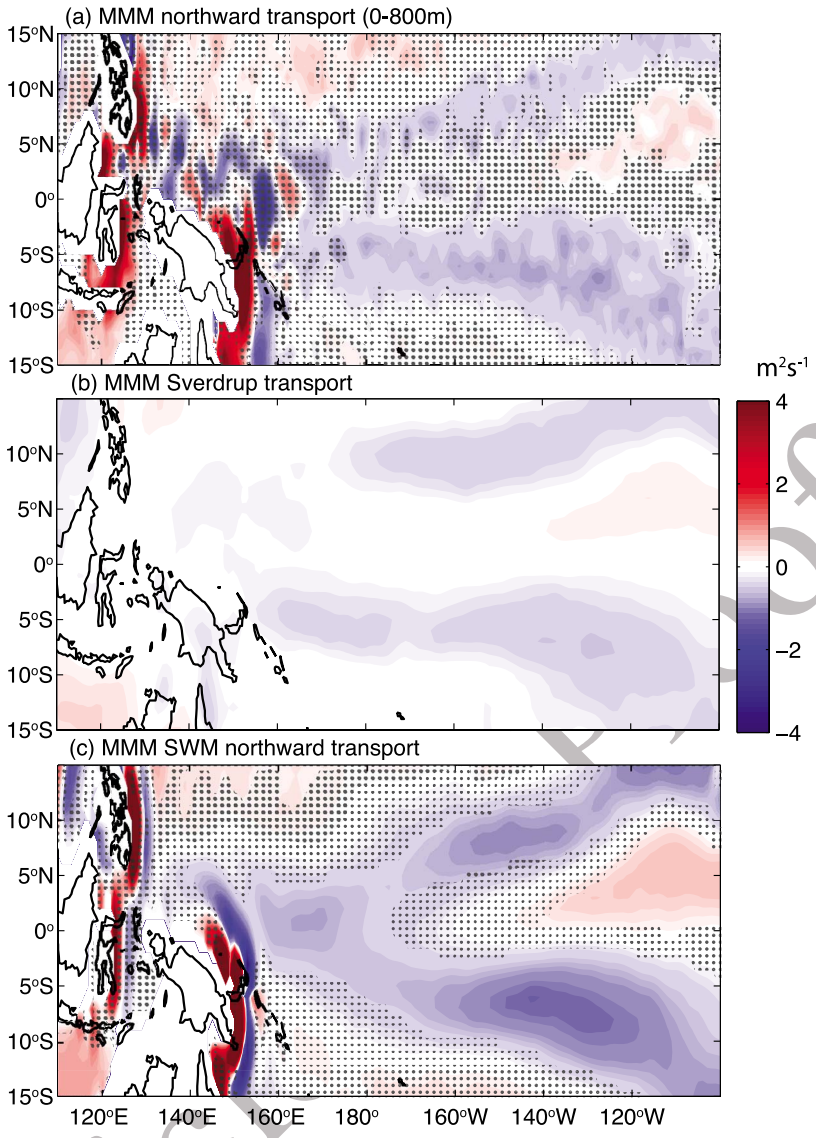


**Figure 4.** Multi model mean change in (a) vertically integrated (0–800 m) meridional velocity for CMIP3 models, (b) Sverdrup transport and (b) meridional velocity from upper layer of shallow water model forced by wind-stress trends from individual models. Shaded areas indicate regions where the mean change is not significant (at 95% level). (Units m2/s.)



influence of the off-equatorial compared to the on-equatorial process is consistent with the multi-model mean EUC projection whereby transport is enhanced over a considerably greater portion of the basin than typical during El Niño events.

[15] To summarise, it would appear that the EUC change is primarily related to an acceleration of the NGCU that feeds the EUC from the south, and a compensating reduction in the southern hemisphere interior pycnocline convergence. This is in turn related to the strong wind stress curl anomaly extending across much of the basin centred at ~7°S. In the northern hemisphere the projected negative curl anomaly is consistent with the weakened southward boundary flow at 9°N. A direct link to changes in the boundary flow closer to the equator and thus to the EUC is complicated by complex circulation pathways that incorporate the ITF. These pathways are dependent on bathymetry that can vary considerably across models. It is plausible that the slowdown at 9°N is connected with the ITF transport reduction and does not have a large impact on the EUC changes.

## 5. Shallow Water Model (SWM)

[16] To test the qualitative arguments presented above we use the projected 21st century wind-stress trends from individual models, to drive a 1½-layer SWM. The model represents a dynamic upper ocean with a motionless deep ocean separated by a thermocline that can vary in depth with time [*McGregor et al.*, 2007]. The model isolates the linear wind-driven response of the upper ocean circulation, and excludes possible buoyancy driven effects.

[17] Figure 4 compares the multi-model mean, depth integrated (0–800 m), meridional velocity projections from the CMIP3 model and the corresponding upper layer SWM results. The SWM contains a relatively crude representation of ocean dynamics. On long timescales it captures the Sverdrup response to the wind field changes (Figure 4b) and

the associated western boundary adjustment. There are some large discrepancies in bathymetry between the SWM and the CMIP3 models. Despite this, the upper ocean response, simulated in the CMIP3 models, is well reproduced by the simple model. Most prominent is the intensification of the northward boundary flow along PNG and a compensating interior southward flow. Substantially weaker northward anomalies are also evident at the western boundary in the northern hemisphere. There is also a compensating increase in the equatorward flow in the interior. The projected negative wind stress curl anomalies at ~7°S and ~10°N (Figure 3a) are thus related to a strengthening of the NGUC and a weakening Mindanao Current together with some degree of interior compensation. The ITF reduction is also reproduced in the SWM, suggesting a significant wind-driven slowdown of the transport between the tropical Pacific and Indian oceans. The positive anomaly connecting the ITF and the Mindanao Current (in both the CMIP3 and SWM) suggests that the reduced ITF is related to the weakened Mindanao Current. As such, the EUC intensification is primarily related to changes in the southern hemisphere circulation.

## 6. Discussion

[18] We examine projections of the EUC and NGCU and explore the reasons behind their simulated increases. In particular, we find a strong projected wind stress curl anomaly to the south of the equator that is consistent with a weakened interior convergence and an enhancement of the NGCU western boundary flow. This pattern of change is essentially unaffected if the near-surface wind-driven layer is removed. This in turn increases the EUC from the western through to the central basin. We would expect the projected reduction in equatorial trade winds to decelerate the STCs [e.g., *Lee and Fukumori*, 2003] and indeed we find that the EUC is projected to weaken slightly by the time it reaches the eastern basin. However some disagreement exists with regard to the projected STC changes. *Luo et al.* [2009] find no consistent change in the projected equatorward meridional convergence and an almost complete compensation between interior and boundary pycnocline convergence. *Wang and Cane* [2011], on the other hand, find a robust weakening of the STC but little evidence of either flow compensation or indeed of robust changes to the western boundary currents. This contradiction appears to stem from the fact that *Wang and Cane* [2011] use a time dependent lower pycnocline that shoals over time, such that changes in boundary flow are offset by reduced vertical extent. Although we do not explicitly examine the STC here we clearly see some degree of compensation between interior and western boundary flow and significant changes to the boundary currents (Figure 4). Here we have not restricted our transport definition to the pycnocline as the boundary currents extend both above and below the pycnocline.

[19] The importance of the wind in driving the projected circulation changes is tested in a SWM, forced with projected wind trends from the CMIP3 models. There is excellent agreement between the linear wind-driven response in the SWM and upper ocean response in the CMIP3 models, with both showing a strong acceleration of the NGCU. *Luo et al.* [2009] note that the projected changes to the EUC may be driven by either wind or buoyancy flux changes that may alter the potential vorticity and thus the pathways of flow feeding into the EUC. Here we have demonstrated that the projected changes are consistent with a purely wind driven response. We note however that there is a robust projected increase in the strength of upper ocean stratification over the tropical ocean [*Capotondi et al.*, 2012]. Further experiments with more sophisticated ocean models would be required to identify the importance of buoyancy effects.

[20] While the wind-related processes described above can explain circulation changes associated with both interannual variability and multi-decadal trends, the causes for the wind changes are not the same. ENSO variability is intimately tied to the zonal equatorial SST gradient and the Bjerknes feedback. The causes for the projected wind changes appear to be very different. The strengthening of the southeast trades is fundamental in driving the projected circulation changes. It is associated with differences in projected warming between the equator and the southeastern Pacific Ocean [*Timmermann et al.*, 2010; *Xie et al.*, 2010]. *Xie et al.* [2010], for example, use an atmospheric model forced (over 2000–2060) with (i) projected SST, with radiative forcing held fixed (ii) evolving radiative forcing, with SST held fixed and (iii) evolving SST and radiative forcing, to examine the mechanisms driving the intensification. Even in the absence of SST changes there is a projected intensification of the southeast trades south of 20S, suggesting that the wind intensification is triggered by changes in radiative forcing but is then amplified and extended equatorward by a wind-evaporation-SST feedback whereby stronger mean winds in the southeast Pacific slow the rate of ocean warming in this region [*Xie et al.*, 2010]. Similar conclusions were used to explain historical changes [*Deser and Phillips*, 2009]. This is a robust result from all climate models. Multiple processes also lead to an enhanced equatorial SST warming in many of the climate models [*DiNezio et al.*, 2009]. The strengthened meridional SST gradient helps to intensify the southeast Trade winds. In addition, the projected weakening of the equatorial winds appears to be related to a slowdown of the atmospheric overturning circulation, driven by the differential sensitivity of atmospheric water vapor increase and radiative cooling to a CO2-induced warming [*Held and Soden*, 2006]. As such the drivers of the projected changes are fundamentally different to those that drive ENSO. Also, given the differences in the oceanic responses, describing the projected changes in the Tropical Pacific as 'EL-Niño-like' as is frequently done, is inappropriate. A number of previous studies that have examined different components of the tropical Pacific climate have similarly found that the projected change is not well described as being El Nino- or La Nina-like [e.g., *van Oldenborgh et al.*, 2005; *Collins*, 2005; *Vecchi et al.*, 2006; *Vecchi and Soden*, 2007; *DiNezio et al.*, 2010].

[21] The projected increase in the NGCU and upper EUC has the potential to enhance entrainment and supply of bio-available iron into the eastern Pacific. At the same time, however, there is an increase in the vertical stratification and a general decrease in the wind driven upwelling along the equator. As such further work is required to understand how these competing effects will affect the iron limited biological systems of the tropical Pacific.

[22] **Acknowledgments.** This project was supported by the *Pacific* Australia Climate Change Science and Adaptation Program a program managed by the Department of Climate Change and Energy Efficiency in collaboration with AusAID, and delivered by the Bureau of Meteorology

and the Commonwealth Scientific and Industrial Research Organisation (CSIRO). This was also partially funded by ANR project ANR-09-BLAN-0233-01; it is a contribution to CLIVAR/SPICE. This project is supported by the Australian Research Council. We would like to thank Antonietta Capotondi and one anonymous reviewer for their valuable comments.

[23] The Editor thanks two anonymous reviewers for assisting with the evaluation of this paper.

## References

Butt, J., and E. Lindstrom (1994), Currents off the east coast of New Ireland, Papua New Guinea, and their relevance to regional undercurrents in the western equatorial Pacific Ocean, *J. Geophys. Res.*, *99*(C6), 12,503–12,514, doi:10.1029/94JC00399.

Capotondi, A., M. A. Alexander, C. Deser, and M. J. McPhaden (2005), Anatomy and decadal evolution of the Pacific subtropical–tropical cells (STCs), *J. Clim.*, *18*(18), 3739–3758, doi:10.1175/JCLI3496.1.

Capotondi, A., M. A. Alexander, N. A. Bond, E. N. Curchitser, and J. Scott (2012), Enhanced upper-ocean stratification with climate change in the CMIP3 models, *J. Geophys. Res.*, doi:10.1029/2011JC007409, in press.

Coale, K. H., S. E. Fitzwater, R. M. Gordon, K. S. Johnson, and R. T. Barber (1996), Control of community growth and export production by upwelled iron in the equatorial Pacific Ocean, *Nature*, *379*(6566), 621–624, doi:10.1038/379621a0.

Collins, M. (2005), El Niño- or La Niña-like climate change?, *Clim. Dyn.*, *24*(1), 89–104, doi:10.1007/s00382-004-0478-x.

Collins, M., et al. (2010), The impact of global warming on the tropical Pacific Ocean and El Niño, *Nat. Geosci.*, *3*(6), 391–397, doi:10.1038/ngeo868.

Cravatte, S., A. Ganachaud, Q.-P. Duong, W. S. Kessler, G. Eldin, and P. Dutrieux (2011), Observed circulation in the Solomon Sea from SADCP data, *Prog. Oceanogr.*, *88*(1–4), 116–130, doi:10.1016/j.pocean.2010.12.015.

Delcroix, T., G. Eldin, M.-H. Radenac, J. Toole, and E. Firing (1992), Variation of the western equatorial Pacific Ocean, 1986–1988, *J. Geophys. Res.*, *97*(C4), 5423–5445, doi:10.1029/92JC00127.

Deser, C., and A. S. Phillips (2009), Atmospheric circulation trends, 1950–2000: The relative roles of sea surface temperature forcing and direct atmospheric radiative forcing, *J. Clim.*, *22*(2), 396–413, doi:10.1175/2008JCLI2453.1.

DiNezio, P. N., A. C. Clement, G. A. Vecchi, B. J. Soden, B. P. Kirtman, and S.-K. Lee (2009), Climate response of the equatorial Pacific to global warming, *J. Clim.*, *22*(18), 4873–4892, doi:10.1175/2009JCLI2982.1.

DiNezio, P., A. Clement, and G. Vecchi (2010), Reconciling differing views of tropical Pacific climate change, *Eos Trans. AGU*, *91*(16), 141, doi:10.1029/2010EO160001.

Feely, R. A., T. Takahashi, R. Wanninkhof, M. J. McPhaden, C. E. Cosca, S. C. Sutherland, and M.-E. Carr (2006), Decadal variability of the air-sea $CO_2$ fluxes in the equatorial Pacific Ocean, *J. Geophys. Res.*, *111*, C08S90, doi:10.1029/2005JC003129.

Ganachaud, A., et al. (2011), Observed and expected changes to the tropical Pacific Ocean, in *Vulnerability of Tropical Pacific Fisheries and Aquaculture to Climate Change*, edited by J. D. Bell, J. E. Johnson, and A. J. Hobday, pp. 101–187, Secr. of the Pac. Community, Noumea, New Caledonia.

Ganachaud, A., A. Sen Gupta, J. N. Brown, K. Evans, C. Maes, L. C. Muir, and F. Graham (2012), Projected changes in the tropical Pacific Ocean of importance to tuna fisheries, *Clim. Change*, in press.

Gouriou, Y., and J. Toole (1993), Mean circulation of the upper layers of the western equatorial Pacific Ocean, *J. Geophys. Res.*, *98*(C12), 22,495–22,520, doi:10.1029/93JC02513.

Held, I. M., and B. J. Soden (2006), Robust responses of the hydrological cycle to global warming, *J. Clim.*, *19*(21), 5686–5699, doi:10.1175/JCLI3990.1.

Huang, B., and Z. Liu (1999), Pacific subtropical-tropical thermocline water exchange in the National Centers for Environmental Prediction ocean model, *J. Geophys. Res.*, *104*(C5), 11,065–11,076, doi:10.1029/1999JC900024.

Irving, D., et al. (2011), Evaluating global climate models for climate change projections in the Pacific island region, *Clim. Res.*, *49*, 169–187, doi:10.3354/cr01028.

Izumo, T. (2005), The equatorial undercurrent, meridional overturning circulation, and their roles in mass and heat exchanges during El Niño events in the tropical Pacific Ocean, *Ocean Dyn.*, *55*(2), 110–123, doi:10.1007/s10236-005-0115-1.

Johnson, G., and M. McPhaden (1999), Interior pycnocline flow from the subtropical to the equatorial Pacific Ocean, *J. Phys. Oceanogr.*, *29*(12), 3073–3089, doi:10.1175/1520-0485(1999)029<3073:IPFFTS>2.0.CO;2.

Kuroda, Y. (2000), Variability of currents off the northern coast of New Guinea, *J. Oceanogr.*, *56*(1), 103–116, doi:10.1023/A:1011122810354.

Lee, T., and I. Fukumori (2003), Interannual-to-decadal variations of tropical-subtropical exchange in the Pacific Ocean: Boundary versus interior pycnocline transports, *J. Clim.*, *16*(24), 4022–4042, doi:10.1175/1520-0442(2003)016<4022:IVOTEI>2.0.CO;2.

Lukas, R., E. Firing, P. Hacker, P. L. Richardson, C. A. Collins, R. Fine, and R. Gammon (1991), Observations of the Mindanao Current during the western equatorial Pacific Ocean circulation study, *J. Geophys. Res.*, *96*(C4), 7089–7104, doi:10.1029/91JC00062.

Luo, Y., L. M. Rothstein, and R.-H. Zhang (2009), Response of Pacific subtropical-tropical thermocline water pathways and transports to global warming, *Geophys. Res. Lett.*, *36*, L04601, doi:10.1029/2008GL036705.

Mackey, D. J., J. E. O'sullivan, and R. J. Watson (2002), Iron in the western Pacific: A riverine or hydrothermal source for iron in the Equatorial Undercurrent?, *Deep Sea Res., Part I*, *49*(5), 877–893, doi:10.1016/S0967-0637(01)00075-9.

McGregor, S., N. J. Holbrook, and S. B. Power (2007), Interdecadal sea surface temperature variability in the equatorial Pacific Ocean. Part I: The role of off-equatorial wind stresses and oceanic Rossby waves, *J. Clim.*, *20*, 2643–2658, doi:10.1175/JCLI4145.1.

McPhaden, M. J. (1993), Trade wind fetch related variations in Equatorial Undercurrent depth, speed, and transport, *J. Geophys. Res.*, *98*(C2), 2555–2559, doi:10.1029/92JC02683.

Meehl, G. A., C. Covey, T. Delworth, M. Latif, B. McAvaney, J. F. Mitchell, R. J. Stouffer, and K. E. Taylor (2007), The WCRP CMIP3 multimodel dataset, *Bull. Am. Meteorol. Soc.*, *88*, 1383–1394, doi:10.1175/BAMS-88-9-1383.

Rayner, N. A., D. E. Parker, E. B. Horton, C. K. Folland, L. V. Alexander, D. P. Rowell, E. C. Kent, and A. Kaplan (2003), Global analyses of sea surface temperature, sea ice, and night marine air temperature since the late nineteenth century, *J. Geophys. Res.*, *108*(D14), 4407, doi:10.1029/2002JD002670.

Ryan, J. P., I. Ueki, Y. Chao, H. Zhang, P. S. Polito, and F. P. Chavez (2006), Western Pacific modulation of large phytoplankton blooms in the central and eastern equatorial Pacific, *J. Geophys. Res.*, *111*, G02013, doi:10.1029/2005JG000084.

Sen Gupta, A., A. Santoso, A. S. Taschetto, C. C. Ummenhofer, J. Trevena, and M. H. England (2009), Projected changes to the Southern Hemisphere ocean and sea ice in the IPCC AR4 climate models, *J. Clim.*, *22*(11), 3047–3078, doi:10.1175/2008JCLI2827.1.

Sen Gupta, D. A., D. L. C. Muir, D. J. N. Brown, D. S. J. Phipps, D. P. J. Durack, D. D. Monselesan, and D. S. E. Wijffels (2012), Climate drift in the CMIP3 models, *J. Clim.*, doi:10.1175/JCLI-D-11-00312.1, in press.

Timmermann, A., S. McGregor, and F. F. Jin (2010), Wind effects on past and future regional sea level trends in the southern Indo-Pacific, *J. Clim.*, *23*(16), 4429–4437, doi:10.1175/2010JCLI3519.1.

Tsuchiya, M., R. Lukas, R. A. Fine, E. Firing, and E. Lindstrom (1989), Source waters of the Pacific equatorial undercurrent, *Prog. Oceanogr.*, *23*(2), 101–147, doi:10.1016/0079-6611(89)90012-8.

Ueki, I. (2003), Observation of current variations off the New Guinea coast including the 1997–1998 El Niño period and their relationship with Sverdrup transport, *J. Geophys. Res.*, *108*(C7), 3243, doi:10.1029/2002JC001611.

Uppala, S. M., et al. (2005), The ERA-40 re-analysis, *Q. J. R. Meteorol. Soc.*, *131*(612), 2961–3012, doi:10.1256/qj.04.176.

van Oldenborgh, G. J., S. Philip, M. Collins, et al. (2005), El Niño in a changing climate: A multi-model study, *Ocean Sci. Discuss.*, *2*(3), 267–298, doi:10.5194/osd-2-267-2005.

Vecchi, G. A., and B. J. Soden (2007), Global warming and the weakening of the tropical circulation, *J. Clim.*, *20*(17), 4316–4340, doi:10.1175/JCLI4258.1.

Vecchi, G., B. Soden, A. Wittenberg, I. Held, A. Leetmaa, and M. Harrison (2006), Weakening of tropical Pacific atmospheric circulation due to anthropogenic forcing, *Nature*, *441*(7089), 73–76, doi:10.1038/nature04744.

Wang, D., and M. A. Cane (2011), Pacific shallow meridional overturning circulation in a warming climate, *J. Clim.*, *24*(24), 6424–6439, doi:10.1175/2011JCLI4100.1.

Wijffels, S. E. (1993), Exchanges between hemispheres and gyres: A direct approach to the mean circulation of the equatorial Pacific, PhD thesis, Woods Hole Oceanogr. Inst., Woods Hole, Mass.

Xie, S. P., C. Deser, G. A. Vecchi, J. Ma, H. Teng, and A. T. Wittenberg (2010), Global warming pattern formation: Sea surface temperature and rainfall, *J. Clim.*, *23*(4), 966–986, doi:10.1175/2009JCLI3329.1.